

1 **Running head:** ???

2 Cranial morphological disparity within the
3 adaptive radiation of tenrecs (Afrosoricida,
4 Tenrecidae) is no greater than expected by
5 chance

6 Sive Finlay^{1,2,*} and Natalie Cooper^{1,2}

7 ¹ School of Natural Sciences, Trinity College Dublin, Dublin 2, Ireland.

8 ² Trinity Centre for Biodiversity Research, Trinity College Dublin, Dublin 2, Ireland.

9 *sfinlay@tcd.ie; Zoology Building, Trinity College Dublin, Dublin 2, Ireland.

10 Fax: +353 1 6778094; Tel: +353 1 896 2571.

11 **Keywords:** disparity, morphology, geometric morphometrics, tenrecs,
12 golden moles adaptive radiation

¹³ **Abstract**

14 Introduction

15 Adaptive radiations, "evolutionary divergence of members of a single
16 phylogenetic lineage into a variety of different adaptive forms" (Futuyma
17 1998, cited by Losos, 2010) have long-attracted the interests and attentions
18 of naturalists. Some of the most famous examples include Darwin's
19 finches, cichlid fish and Caribbean *Anolis* lizards (Gavrillets & Losos, 2009).
20 These groups exhibit great variety in both species richness and
21 phenotypic diversity. However, taxonomic diversity does not necessarily
22 correlate with phenotypic variety (Ruta et al., 2013; Hopkins, 2013) and
23 clades that have exceptional phenotypic diversity can still be regarded as
24 adaptive radiations even if they are not taxonomically diverse. Therefore,
25 to determine whether a clade has adaptively radiated it is important to
26 test whether it exhibits exceptional (i.e. greater than expected by chance)
27 morphological and ecological diversity (Losos & Mahler, 2010). However,
28 few adaptive radiations have been characterised in this way.

29 Phenotypic diversity is commonly measured as morphological
30 disparity; the diversity of organic form (Foote, 1997; Erwin, 2007)). There
31 is no single definition of disparity and it can be calculated in many ways
32 including measures of morphospace occupation (e.g. Goswami et al., 2011;
33 Brusatte et al., 2008) and rate-based approaches that assess the amount of
34 directed change away from an ancestor (O'Meara et al., 2006; Price et al.,
35 2013). Analyses of disparity can be apply these alternative approaches
36 depending on whether you are interested in current patterns of
37 morphological diversity or the rate at which they accumulate through
38 time.

39 Here we investigate current patterns of morphological disparity in

40 tenrecs (Afrosoricida, Tenrecidae) to determine whether they represent an
41 adaptive radiation sensu (Losos & Mahler, 2010). Tenrecs are comprised of
42 34 species, 31 of which are endemic to Madagascar (Olson, 2013). From a
43 single common ancestor (Asher & Hofreiter, 2006), Malagasy tenrecs
44 diversified into a wide variety of descendant species which convergently
45 resemble distantly related insectivore mammals such as shrews (*Microgale*
46 tenrecs), moles (*Oryzorictes* tenrecs) and hedgehogs (*Echinops*, *Setifer*
47 tenrecs) (Eisenberg & Gould, 1969).

48 Tenrecs are often cited as an example of an adaptively radiated family
49 which exhibits exceptional morphological diversity (Soarimalala &
50 Goodman, 2011; Olson & Goodman, 2003; Eisenberg & Gould, 1969).
51 However, this apparent exceptional diversity is based on subjective
52 comparisons to other groups and it has not been tested quantitatively. If
53 tenrecs are exceptionally morphologically diverse then there are two
54 predictions; tenrecs are more morphologically disparate than expected by
55 chance and they are significantly more diverse than their nearest relatives,
56 the golden moles (Afrosoricida, Chrysochloridae).

57 Using the most complete morphological data set of tenrecs and golden
58 moles to date we apply geometric morphometric analyses (Rohlf &
59 Marcus, 1993; Zelditch et al., 2012) to quantify morphological disparity
60 among our species. Our results indicate that, on average, tenrecs are more
61 phenotypically diverse than their closest relatives but their morphological
62 diversity is no greater than that which is expected to evolve by chance.
63 Therefore, under strict definitions, their designation as an exceptional
64 adaptive radiation may need to be reconsidered.

65 These findings highlight the vital importance of testing our common,

66 but often erroneous, expectations about patterns of morphological
67 diversity in adaptively radiated groups.

68 **Materials and Methods**

69 **Data collection**

70 **Morphological data collection**

71 One of us (SF) photographed cranial specimens of tenrecs and golden
72 moles at the Natural History Museum London (NHML), the Smithsonian
73 Institute Natural History Museum (SI), the American Museum of Natural
74 History (AMNH), Harvard's Museum of Comparative Zoology (MCZ)
75 and the Field Museum of Natural History, Chicago (FMNH). We
76 photographed the specimens with a Canon EOS 650D camera fitted with
77 an EF 100mm f/2.8 Macro USM lens using a standardised procedure to
78 minimise potential error (see supplementary material for details).

79 We collected pictures of the skulls in dorsal, ventral and lateral views
80 (right side of the skull) and of the outer (buccal) side of the right
81 mandibles. A full list of museum accession numbers and access to the
82 images can be found in the supplementary material.

83 In total we collected pictures from 182 skulls in dorsal view (148
84 tenrecs and 34 golden moles) and 181 mandibles in lateral view (147
85 tenrecs and 34 golden moles), representing 31 species of tenrec (out of the
86 total 34 in the family) and 12 species of golden moles (out of a total of 21
87 in the family (Asher et al., 2010)). We used the taxonomy of Wilson and
88 Reeder (2005) supplemented with more recent sources (IUCN, 2012;

89 Olson, 2013) to identify our specimens.

90 We used a combination of both landmarks (type 2 and type 3,
91 (Zelditch et al., 2012)) and semilandmarks to characterise the shapes of
92 our specimens. Our landmarks (points) and semilandmarks (outline
93 curves) used to represent shape variation in the dorsal skulls and
94 mandibles are depicted in Figures 1 and 2 respectively. Corresponding
95 landmark definitions for each view are in tables 1 and 2. We also placed
96 landmarks and semilandmarks on photographs of ventral and lateral skull
97 views, details can be found in the supplementary material. We digitised
98 all landmarks and semilandmarks in tpsDIG, version 2.17 (Rohlf, 2013).

99 We re-sampled the outlines to a standard number of evenly spaced
100 points which were the minimum number required to represent each
101 outline accurately (MacLeod, 2013, details in supplementary material). We
102 used TPSUtil (Rohlf, 2012) to create sliders files (Zelditch et al., 2012) to
103 define which points were semilandmarks. We conducted all subsequent
104 analyses in R version 3.0.2 (R Development Core Team, 2013) within the
105 geomorph package (Adams et al., 2013). We used the gpagen function to
106 run a general Procrustes alignment (REFS) of the landmark coordinates
107 while sliding the semilandmarks by minimising procrustes distance rather
108 than bending energy (REFS). We used these Procrustes-aligned
109 coordinates of all species (n=43) to calculate average shape values for each
110 species which we then used for a principal components (PC) analysis
111 (REFS) with the plotTangentSpace function (Adams et al., 2013).

Phylogeny

Instead of basing our analyses on individual trees and assuming that their topologies were known without error (e.g. Ruta et al., 2013; Foth et al., 2012; Brusatte et al., 2008; Harmon et al., 2003) we used a distribution of 101 pruned phylogenies derived from the randomly resolved mammalian supertrees in (Kuhn et al., 2011).

Eight species (six *Microgale* tenrecs and two golden moles) in our morphological data were not in the phylogenies. Phylogenetic relationships among the *Microgale* have not been resolved more recently than the (Kuhn et al., 2011) analysis, therefore we added the additional *Microgale* species at random to the *Microgale* genus within each phylogeny (Revell, 2012). We could not use the same approach to add the two missing golden mole species because they were the only representatives of their respective genera within our data. Therefore we randomly added these species to the common ancestral node (using the findMRCA function in phytools (Revell, 2012)) of all golden moles within each phylogeny. Adding these extra species to the phylogenies created polytomies which we resolved arbitrarily using zero-length branches (Paradis et al., 2004). We calculated pairwise phylogenetic distances among species using the cophenetic function (R Development Core Team, 2013).

Analyses

Disparity calculations

We calculated morphological disparity separately for golden moles and tenrecs in each of the morphological datasets. We used the PC axes which

136 accounted for 95% of the cumulative variation to calculate four disparity
137 metrics; the sum and product of the range and variance of morphospace
138 occupied by each family (Brusatte et al., 2008; Foth et al., 2012; Ruta et al.,
139 2013). We also calculated morphological disparity directly from the
140 Procrustes-superimposed shape data (Zelditch et al., 2012). Disparity is
141 expected to be higher in larger groups (REFS). Therefore we repeated our
142 disparity comparisons between the two families using rarefaction (see
143 supplementary material) to confirm that observed differences in disparity
144 between the two groups were not artefacts of differences in sample size.

145 To test whether tenrecs are more morphologically disparate than
146 expected by chance, we simulated shape evolution (Harmon et al., 2008) of
147 the species-average, Procrustes-superimposed shape coordinates of each
148 tenrec species across our distribution of phylogenies under a Brownian
149 Motion (BM) model (1000 simulations on each of 101 phylogenies pruned
150 to include tenrec species only). We ran a principal components analysis on
151 each of the simulations and used the PC axes which accounted for 95% of
152 the cumulative variation to calculate disparity metrics.

153 We compared the observed disparity measure to the corresponding
154 distribution of values and used a two-tailed test to determine whether the
155 observed (true) disparity measures were more or less than expected by
156 chance.

157 The majority of tenrecs (19 out of 31 in our data) are members of the
158 *Microgale* (shrew-like) genus which is notable for its relatively low
159 phenotypic diversity (Soarimalala & Goodman, 2011; Jenkins, 2003) and
160 may mask signals of high disparity among other tenrecs. To test this we
161 repeated our simulations of shape evolution excluding *Microgale* species.

162 This reduced our data set for tenrecs from 31 to 12 species.

163 To test whether tenrecs are more disparate than their nearest relatives,
164 we used a non parametric MANOVA (Anderson, 2001) to compare
165 morphospace occupation between the two groups (REFS?).

166 **Results**

167 **Morphological disparity in tenrecs**

168 We compared observed disparity to calculations of disparity from BM
169 simulations of shape data (1,000 simulations on each of 101 phylogenies).
170 For each metric of disparity in both the dorsal skulls (table 3) and
171 mandibles (table 4), the true (observed) values were significantly lower
172 than expected compared to the distribution of simulated values. We also
173 found significantly lower disparity than expected by chance in both the
174 ventral and lateral skull views (supplementary material).

175 Removing the phenotypically similar *Microgale* tenrecs did not
176 qualitatively affect our results; the non-*Microgale* tenrecs still show
177 significantly lower phenotypic disparity than expected by chance
178 (simulation results in the supplementary material).

179 **Morphological disparity in tenrec and golden moles**

180 Figures 3 and 4 depict the morphospace plots derived from our principal
181 components analyses of average Procrustes-superimposed shape
182 coordinates for each species in our skull and mandible data respectively.
183 We used the principal components axes which accounted for 95% of the

184 cumulative variation ($n = 6$ axes for the dorsal skulls analysis and $n = 11$
185 axes for the mandibles) to calculate the disparity of each family.

186 There was agreement among all of our disparity metrics that tenrecs
187 have more diverse dorsal skull shapes than golden moles and the two
188 families occupy significantly different areas of morphospace
189 (npMANOVA, $F = 59.34$, $R^2 = 0.59$, $p = 0.001$).

190 Unexpectedly, our analyses of disparity in mandible shape yielded the
191 opposite result; golden moles have higher disparity in the shape of their
192 mandibles than tenrecs and they occupy significantly different areas of
193 morphospace (npMANOVA $F = 59.34$, $R^2 = 0.59$, $p = 0.001$)

194 However, this result may be an artefact of the relatively low phenotypic
195 diversity within *Microgale* tenrecs. Golden moles and non-*Microgale*
196 tenrecs occupy significantly different areas of morphospace (npMANOVA
197 $F = 31.6$, $R^2 = 0.59$, $p = 0.001$). However, the overall differences in
198 morphospace occupation are only supported by some of the disparity
199 metrics. When disparity is calculated as the product of variance or
200 product of ranges, golden moles have higher disparity than non-*Microgale*.
201 In contrast, there is no significant difference between the two groups
202 when disparity is measured as the sum of ranges or the sum of variance.

203 Discussion

204 Our findings provide new insights into phenotypic diversity within the
205 tenrec family. Contrary to previous suggestions (e.g. Eisenberg & Gould,
206 1969; Olson, 2013), tenrecs do not appear to be exceptional in their
207 morphological diversity. They do seem to be more morphologically

208 disparate than their closest relatives but only in skull morphology; the
209 opposite is true when we look at mandible morphology (figure 4). Our
210 results illustrate the vital importance of applying quantitative methods to
211 test assumptions about morphological diversity.

212 Tenrecs are evidently a diverse group, both phenotypically and
213 ecologically. Body sizes of extant tenrecs span three orders of magnitude
214 (2.5 to >2,000g) which is a greater range than all other Families, and most
215 Orders, of living mammals (Olson & Goodman, 2003). Within this vast
216 size range there is striking morphological diversity, from the spiny
217 *Echinops*, *Setifer* and striking *Hemicentetes* to the shrew-like *Microgale*.
218 Furthermore, tenrecs inhabit a variety of ecological niches and habitats
219 including terrestrial, arboreal, semi-aquatic and semi-fossorial forms
220 (REFS).

221 However, our results cast doubt over whether the evident diversity
222 within the tenrec family should be considered to be an adaptive radiation.
223 Phenotypic and ecological divergences within a clade are not surprising;
224 most clades have at least small levels of disparity so, when it comes to
225 identifying adaptive radiations, it's important to identify clades which are
226 exceptional in their diversity (Losos & Mahler, 2010). Here we have
227 presented the first quantitative investigation of morphological disparity in
228 tenrecs and our results suggest that perhaps phenotypic variation in
229 tenrecs is not the product of an adaptive radiation in the strict sense of its
230 definition.

231 Although tenrecs are not more morphologically diverse than expected
232 by chance, they do show greater cranial disparity than their nearest
233 relatives. The discrepancies between our analyses of cranial and mandible

234 disparity could reflect derive from factors associated with the modularity
235 of morphological evolution.

236 There is strong evidence that morphological variation in skulls and
237 mandibles is derived from differential evolution of integrated
238 developmental modules (reviewed by Klingenberg, 2013). For example,
239 there seems to be two primary modules in the mouse mandible; an
240 alveolar part which holds the teeth and the ascending ramus for muscle
241 attachment and which articulates with the skull (Klingenberg, 2008).
242 Geometric shape covariation is stronger within rather than between these
243 modules.

244 Our landmarks and curves for the mandibles (figure 2, table 2) include
245 aspects of variation in the dentition but they focus particular attention on
246 the ascending ramus (condyloid, condylar and angular processes).
247 Therefore the higher morphological disparity in golden mole mandibles
248 most likely reflects greater variation in the shape of the muscle attachment
249 areas of the mandible. In contrast it proved impossible to position reliable
250 landmarks on the corresponding articulation areas of the skull in lateral
251 view (see supplementary).

252 If variation in muscle attachment/articulation sites is driving
253 morphological disparity in mandibles, it is not clear why golden moles
254 should have more disparate articular rami than tenrecs.

255 While our findings cast doubt on the designation of tenrecs as an
256 adaptive radiation sensu (Losos & Mahler, 2010), there are certain caveats
257 to consider which could modify the interpretation of our results.

258 Phenotypic variation can evolve for reasons other than adaptive
259 radiation. Therefore, to describe phenotypic divergence as the product of

260 an adaptive radiations requires exceptional morphological diversity in
261 traits which have specific and proven adaptive significance (Losos &
262 Mahler, 2010). The evolution of cranial shape (both upper skull and
263 mandible), particularly dental morphology, has obvious correlations with
264 dietary specialisations (REFS) and occupation of specific ecological niches
265 (REFS).

266 Considering the wide ecological diversity of our study species; the
267 fossorial golden moles and semi-fossorial, arboreal, terrestrial and
268 semi-aquatic tenrecs (REFS) it is reasonable to expect that variation in
269 cranial shape should be an adaptive characteristic which allows the
270 animals to survive in their divergent niches. Therefore quantifying the
271 diversity of cranial morphology is a reasonable method of assessing the
272 significance of morphological variety within the context of identifying an
273 adaptive radiation.

274 Cranial shape similarities are commonly used to delineate species
275 boundaries (REFS) or for cross-taxonomic comparative studies of
276 phenotypic (dis)similarities (REFS). However, disparity studies are
277 inevitably constrained to be measures of diversity within specific traits
278 rather than overall morphology (Roy & Foote, 1997). Therefore it is
279 possible that other morphological proxies of phenotype; analyses of linear
280 measurements and/or discrete characters of either cranial or post-cranial
281 morphologies could yield different results.

282 However, the results of (Foth et al., 2012) are encouraging. In an
283 analysis of morphological disparity in pterosaurs, they found that
284 disparity calculations based on geometric morphometric characterisation
285 of skull shape yielded broadly similar results compared to analyses of

286 whole-skeleton discrete characters and limb proportion data sets.
287 Therefore the disparity patterns we find here based on geometric
288 morphometric analyses of cranial shape most likely represent
289 approximations of disparity which are accurate for morphological
290 diversity in the clades.

291 **Acknowledgements**

292 We thank the members of NERD club for insightful discussions and the
293 museum staff and curators for their support and access to collections.
294 Funding was provided by an Irish Research Council EMBARK Initiative
295 Postgraduate Scholarship (SF) and the European Commission CORDIS
296 Seventh Framework Programme (FP7) Marie Curie CIG grant. Proposal
297 number: 321696 (NC, SF)

298 **References**

- 299 Adams, D., Otárola-Castillo, E. & Paradis, E. 2013. geomorph: an r
300 package for the collection and analysis of geometric morphometric
301 shape data. *Methods in Ecology and Evolution* **4**: 393–399.
302 10.1111/2041-210X.12035.
- 303 Anderson, M. 2001. A new method for non-parametric multivariate
304 analysis of variance. *Austral Ecology* **26**: 32–46.
305 10.1111/j.1442-9993.2001.01070.pp.x.
- 306 Asher, R. & Hofreiter, M. 2006. Tenrec phylogeny and the noninvasive
307 extraction of nuclear DNA. *Systematic Biology* **55**: 181–194.

- 308 Asher, R.J., Maree, S., Bronner, G., Bennett, N., Bloomer, P., Czechowski,
309 P., Meyer, M. & Hofreiter, M. 2010. A phylogenetic estimate for golden
310 moles (Mammalia, Afrotheria, Chrysochloridae). *BMC Evolutionary*
311 *Biology* **10**: 1–13.
- 312 Brusatte, S., Benton, M., Ruta, M. & Lloyd, G. 2008. Superiority,
313 competition and opportunism in the evolutionary radiation of
314 dinosaurs. *Science* **321**: 1485–1488.
- 315 Eisenberg, J.F. & Gould, E. 1969. The Tenrecs: A Study in Mammalian
316 Behaviour and Evolution. *Smithsonian Contributions to Zoology* **27**: 1–152.
- 317 Erwin, D. 2007. Disparity: morphological pattern and developmental
318 context. *Palaeontology* **50**: 57–73.
- 319 Foote, M. 1997. The evolution of morphological diversity. *Annual Review of*
320 *Ecology and Systematics* **28**: 129–152.
- 321 Foth, C., Brusatte, S. & Butler, R. 2012. Do different disparity proxies
322 converge on a common signal? Insights from the cranial morphometrics
323 and evolutionary history of *Pterosauria* (Diapsida: Archosauria). *Journal*
324 *of Evolutionary Biology* **25**: 904–915. 10.1111/j.1420-9101.2012.02479.x.
- 325 Gavrillets, S. & Losos, J. 2009. Adaptive radiation: contrasting theory with
326 data. *Science* **323**: 732–736. 10.1126/science.1157966.
- 327 Goswami, A., Milne, N. & Wroe, S. 2011. Biting through constraints:
328 cranial morphology, disparity and convergence across living and fossil
329 carnivorous mammals. *Proceedings of the Royal Society B: Biological*
330 *Sciences* **278**: 1831–1839. 10.1098/rspb.2010.2031.

- 331 Harmon, L., Schulte, J., Larson, A. & Losos, J.B. 2003. Tempo and mode of
332 evolutionary radiation in iguanian lizards. *Science* **301**: 961–964.
- 333 Harmon, L., Weir, J., Brock, C., Glor, R. & Challenger, W. 2008. GEIGER:
334 investigating evolutionary radiations. *Bioinformatics* **24**: 129–131.
- 335 Hopkins, M. 2013. Decoupling of taxonomic diversity and morphological
336 disparity during decline of the Cambrian trilobite family *Pterocephaliidae*.
337 *Journal of Evolutionary Biology* **26**: 1665–1676. 10.1111/jeb.12164.
- 338 IUCN 2012. International Union for Conservation of Nature.
- 339 Jenkins, P. 2003. *Microgale, shrew tenrecs*, pp. 1273–1278. The University of
340 Chicago Press, Chicago.
- 341 Klingenberg, C. 2008. Morphological integration and developmental
342 modularity. *Annual review of ecology, evolution, and systematics* **39**:
343 115–132.
- 344 Klingenberg, C. 2013. Cranial integration and modularity: insights into
345 evolution and development from morphometric data. *Hystrix, the Italian*
346 *Journal of Mammalogy* **24**: 43–58.
- 347 Kuhn, T., Mooers, A. & Thomas, G. 2011. A simple polytomy resolver for
348 dated phylogenies. *Methods in Ecology and Evolution* **2**: 427–436.
349 10.1111/j.2041-210X.2011.00103.x.
- 350 Losos, J. 2010. Adaptive radiation, ecological opportunity, and
351 evolutionary determinism. American Society of Naturalists E. O. Wilson
352 Award Address. *The American Naturalist* **175**: 623–639. 10.1086/652433.

- 353 Losos, J.B. & Mahler, D. 2010. *Adaptive radiation: the interaction of ecological*
354 *opportunity, adaptation and speciation*, chap. 15, pp. 381–420. Sinauer
355 Association, Sunderland, MA.
- 356 MacLeod, N. 2013. Landmarks and semilandmarks: Difference without
357 meaning and meaning without difference.
- 358 Olson, L. & Goodman, S. 2003. *Phylogeny and biogeography of tenrecs*, pp.
359 1235–1242. The University of Chicago Press, Chicago.
- 360 Olson, L.E. 2013. Tenrecs. *Current Biology* **23**: R5–R8.
- 361 O'Meara, B., Ané, C., Sanderson, M. & Wainwright, P. 2006. Testing for
362 different rates of continuous trait evolution using likelihood. *Evolution*
363 **60**: 922–933. 10.1111/j.0014-3820.2006.tb01171.x.
- 364 Paradis, E., Claude, J. & Strimmer, K. 2004. Ape: Analyses of
365 Phylogenetics and Evolution in R language. *Bioinformatics* **20**: 289–290.
366 10.1093/bioinformatics/btg412.
- 367 Price, S., Tavera, J., Near, T. & Wainwright, P. 2013. Elevated rates of
368 morphological and functional diversification in reef-dwelling haemulid
369 fishes. *Evolution* **67**: 417–428. 10.1111/j.1558-5646.2012.01773.x.
- 370 Revell, L. 2012. phytools: an R package for phylogenetic comparative
371 biology (and other things). *Methods in Ecology and Evolution* **3**: 217–223.
- 372 Rohlf, F. 2012. Tpsutil.
- 373 Rohlf, F. 2013. Tpsdig2 ver 2.17.
- 374 Rohlf, J. & Marcus, L. 1993. A revolution in morphometrics. *Trends in*
375 *Ecology & Evolution* **8**: 129–132.

- 376 Roy, K. & Foote, M. 1997. Morphological approaches to measuring
377 biodiversity. *Trends in Ecology & Evolution* **12**: 277–281.
- 378 Ruta, M., Angielczyk, K., Fröbisch, J. & Benton, M. 2013. Decoupling of
379 morphological disparity and taxic diversity during the adaptive
380 radiation of anomodont therapsids. *Proceedings of the Royal Society B:*
381 *Biological Sciences* **280**: 20131071. 10.1098/rspb.2013.1071.
- 382 Soarimalala, V. & Goodman, S. 2011. *Les petits mammifères de Madagascar*.
383 Guides sur la diversité biologique de Madagascar. Association Vahatra,
384 Antananarivo, Madagascar.
- 385 Team, R.D.C. 2013. R: A language and environment for statistical
386 computing.
- 387 Wilson, D. & Reeder, D. 2005. *Mammal species of the world. A taxonomic and*
388 *geographic reference (3rd ed)*. Johns Hopkins University Press.
- 389 Zelditch, M., Swiderski, D. & Sheets, D. 2012. *Geometric Morphometrics for*
390 *Biologists, second edition*. Academic Press, Elsevier, United States of
391 America.

392 List of Figures

393	1	Landmarks (red points) and curves (blue lines) used to capture the morphological shape of skulls in dorsal view. Curves were re-sampled to the same number of evenly-spaced points. See table X for description of curves and landmarks.	
394		<i>Potamogale</i>	
395		<i>velox</i> (Tenrecidae) skull, accession number: AMNH_51327 . .	20
396			
397	2	Landmarks (red points) and curves (blue lines) used to capture the morphological shape of mandibles. Curves were re-sampled to the same number of evenly-spaced points. See table X for description of curves and landmarks.	
398		<i>Potamogale</i>	
399		<i>velox</i> (Tenrecidae) mandible, accession number: AMNH_51327	21
400			
401	3	Principal components plot of the dorsal skulls' morphospace occupied by tenrecs (red, n=31) and golden moles (black, n=12). Axes are PC1 and PC2 of the average scores from a PCA analysis of mean Procrustes shape coordinates for each species.	22
402			
403	4	Principal components plot of the mandibles' morphospace occupied by tenrecs (red, n=31) and golden moles (black, n=12). Axes are PC1 and PC2 of the average scores from a PCA analysis of mean Procrustes shape coordinates for each species.	
404			
405			
406			
407			
408			
409			
410			
411			
412			

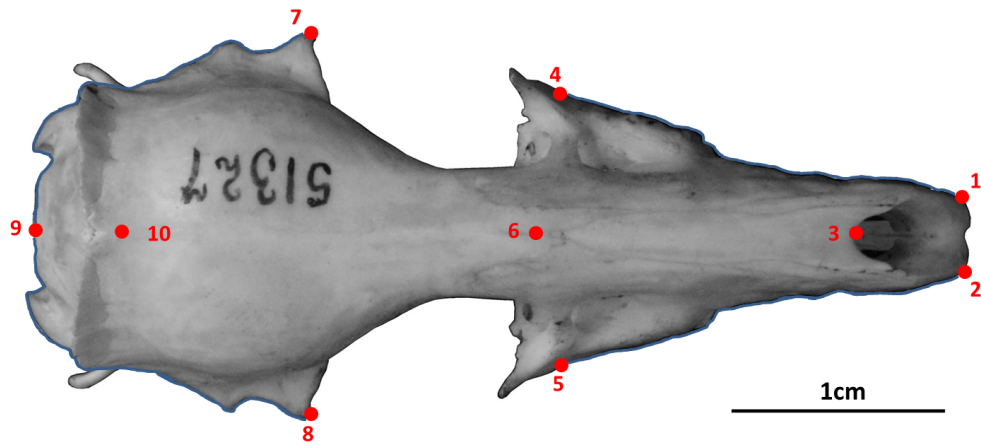


Figure 1: Landmarks (red points) and curves (blue lines) used to capture the morphological shape of skulls in dorsal view. Curves were re-sampled to the same number of evenly-spaced points. See table X for description of curves and landmarks. *Potamogale velox* (Tenrecidae) skull, accession number: AMNH_51327

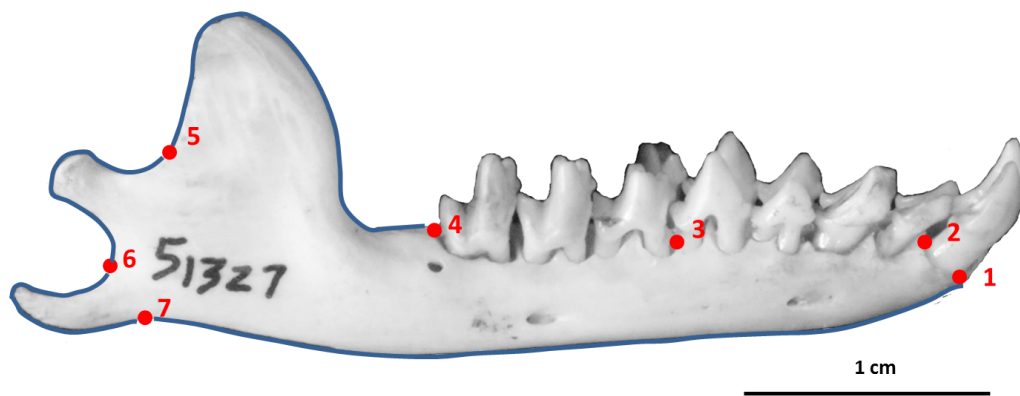


Figure 2: Landmarks (red points) and curves (blue lines) used to capture the morphological shape of mandibles. Curves were re-sampled to the same number of evenly-spaced points. See table X for description of curves and landmarks. *Potamogale velox* (Tenrecidae) mandible, accession number: AMNH_51327

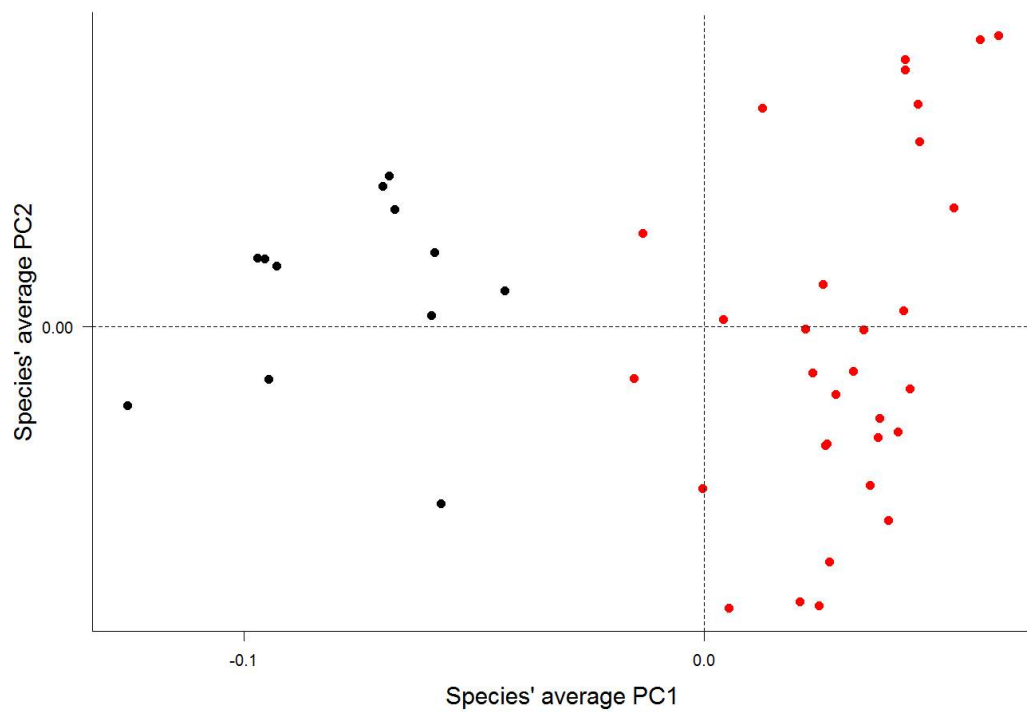


Figure 3: Principal components plot of the dorsal skulls' morphospace occupied by tenrecs (red, $n=31$) and golden moles (black, $n=12$). Axes are PC1 and PC2 of the average scores from a PCA analysis of mean Procrustes shape coordinates for each species.

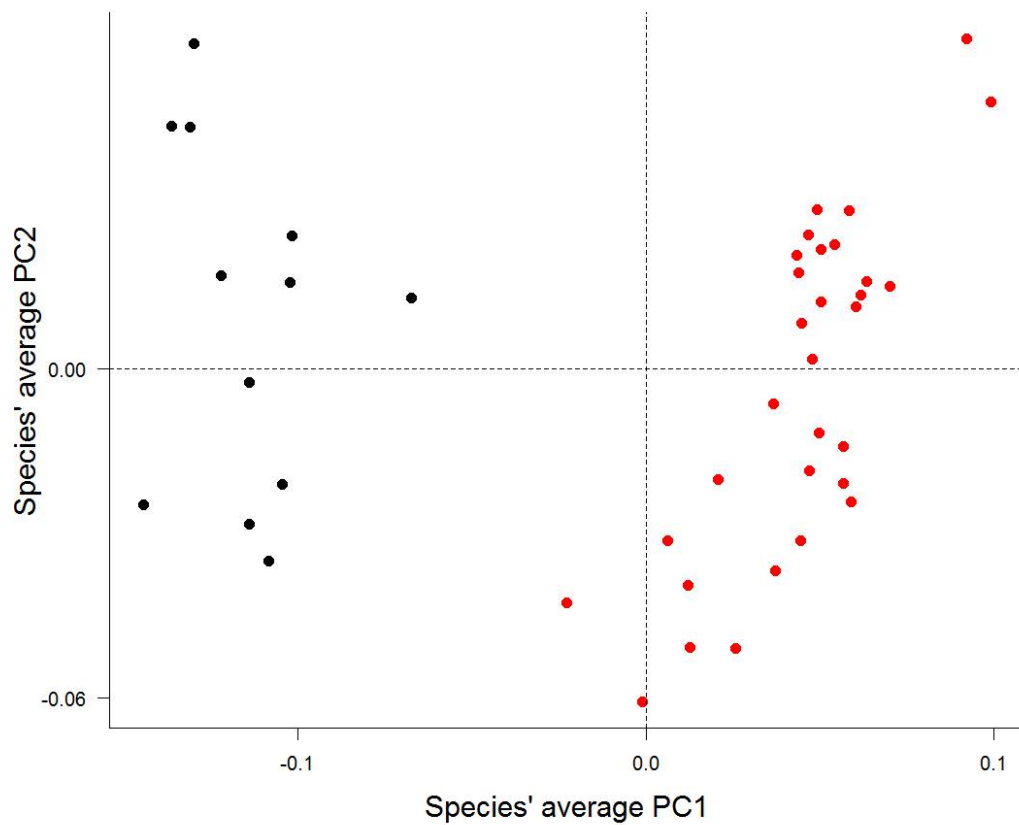


Figure 4: Principal components plot of the mandibles' morphospace occupied by tenrecs (red, n=31) and golden moles (black, n=12). Axes are PC1 and PC2 of the average scores from a PCA analysis of mean Procrustes shape coordinates for each species.

413 List of Tables

414	1	Descriptions of the landmarks (points) and curves (semi-	
415		landmarks) for the skulls in dorsal view (see Figure 1).	25
416	2	Descriptions of the landmarks (points) and curves (semi-	
417		landmarks) for the mandibles in lateral (buccal) view (see	
418		figure 2)	26
419	3	Comparison of observed and simulated disparity measures	
420		for the dorsal skulls analysis; observed (true) disparity mea-	
421		sures, minimum simulated value (sim.min), maximum sim-	
422		ulated value (sim.max), standard deviation of the simulated	
423		values (sdev.sim) and p value comparing the observed dis-	
424		parity measures to the distribution of simulated values) . . .	27
425	4	Comparison of observed and simulated disparity measures	
426		for the mandibles analysis; observed (true) disparity mea-	
427		sures, minimum simulated value (sim.min), maximum sim-	
428		ulated value (sim.max), standard deviation of the simulated	
429		values (sdev.sim) and p value comparing the observed dis-	
430		parity measures to the distribution of simulated values) . . .	28

Table 1: Descriptions of the landmarks (points) and curves (semilandmarks) for the skulls in dorsal view (see Figure 1).

Landmark	Description
1 + 2	Left (1) and right (2) anterior points of the premaxilla
3	Anterior of the nasal bones in the midline
4 + 5	Maximum width of the palate (maxillary) on the left (4) and right (5)
6	Midline intersection between nasal and frontal bones
7 + 8	Widest point of the skull on the left (7) and right (8)
9	Posterior of the skull in the midline
10	Posterior intersection between sagittal and parietal sutures
Curve A (12 points)	Outline of the braincase on the left side, between landmarks 9 and 7 (does not include visible features from the lower (ventral) side of the skull)
Curve B (10 points)	Outline of the palate on the left side, between landmarks 4 and 1 (outline of the rostrum only, not the shape of the teeth)
Curve C (12 points)	Outline of the braincase on the right side, between landmarks 9 and 8 (does not include visible features from the lower (ventral) side of the skull)
Curve D (10 points)	Outline of the palate on the right side, between landmarks 5 and 2 (outline of the rostrum only, not the shape of the teeth)

Table 2: Descriptions of the landmarks (points) and curves (semilandmarks) for the mandibles in lateral (buccal) view (see figure 2)

Landmark	Description
1	Anterior of the alveolus of the first incisor
2	Posterior of the alveolus of the first incisor
3	Anterior of the alveolus of the first molar
4	Posterior of the alveolus of the last molar
5	Maximum curvature between the coronoid and condylar processes
6	Maximum curvature between the condylar and angular processes
7	Maximum curvature between the angular process and the horizontal ramus
Curve A	Condylar process (between landmarks 4 and 5, 15 points)
Curve B	Condylar process (between landmarks 5 and 6, 15 points)
Curve C	Angular process (between landmarks 6 and 7, 15 points)
Curve D	Base of the jaw (between landmarks 7 and 1, 12 points)

Table 3: Comparison of observed and simulated disparity measures for the dorsal skulls analysis; observed (true) disparity measures, minimum simulated value (sim.min), maximum simulated value (sim.max), standard deviation of the simulated values (sdev.sim) and p value comparing the observed disparity measures to the distribution of simulated values)

Disparity metric	Observed	Sim.min	Sim.max	Sdev.sim	p value
Sum of Variance	0.0026	23768.99	352047.7	21020.33	0
Product of Variance	0.00014	1145.99	62118.9	1590.39	0
Sum of Ranges	0.56	1464.11	3090.03	167.77	0
Product of Ranges	0.05	141.0053	877.23	45.29	0
ZelditchMD	0.003	30629.96	422263.07	28276.87	0

Table 4: Comparison of observed and simulated disparity measures for the mandibles analysis; observed (true) disparity measures, minimum simulated value (sim.min), maximum simulated value (sim.max), standard deviation of the simulated values (sdev.sim) and p value comparing the observed disparity measures to the distribution of simulated values)

Disparity metric	Observed	Sim.min	Sim.max	Sdev.sim	p value
Sum of Variance	0.0032	23459.28	286827.19	20915.32	0
Product of Variance	0.000189	1173.95	286827.19	3346.28	0
Sum of Ranges	0.676	1212.44	2996.77	170.86	0
Product of Ranges	0.0639	151.54	1520.68	60.51	0